Letter

Attosecond entangled photons from two-photon decay of metastable atoms: A source for attosecond experiments and beyond

Yimeng Wang [1,*] Siddhant Pandey [1] Chris H. Greene [1,2] and Niranjan Shivaram [1,2,†]

[1]*Department of Physics and Astronomy, Purdue University, West Lafayette, Indiana 47907, USA*

[2]*Purdue Quantum Science and Engineering Institute, Purdue University, West Lafayette, Indiana 47907, USA*

(Received 3 June 2022; accepted 17 August 2022; published 6 September 2022)

We propose the generation of attosecond entangled biphotons in the extreme-ultraviolet regime by two-photon decay of a metastable atomic state as a source similar to spontaneous parametric down-conversion photons. The $1s2s\ ^1S_0$ metastable state in helium decays to the ground state by the emission of two energy-time entangled photons with a photon bandwidth equal to the total energy spacing of 20.62 eV. This results in a pair correlation time in the attosecond regime making these entangled photons a highly suitable source for attosecond pump-probe experiments. The biphoton generation rate from a direct four-photon excitation of helium at 240 nm is calculated and used to assess some feasible schemes to generate these biphotons. Possible applications of entangled biphotons in attosecond timescale experiments, and a discussion of their potential to reach the zeptosecond regime are presented.

DOI: 10.1103/PhysRevResearch.4.L032038

Quantum entanglement is a fascinating quantum phenomenon that has no classical analog [1]. Entanglement is at the heart of quantum information science, quantum sensing, quantum enhanced imaging and spectroscopy, and other emerging quantum technologies. Entanglement of photons has particularly played an important role in many areas of basic and applied research that leverage the quantum advantage. For example, entangled photons have been used in nonlinear spectroscopy [2–4] which goes beyond the time-frequency uncertainty limit [5–7]; moreover, a linear (rather than quadratic) scaling of two-photon absorption rates versus intensity is observed with entangled photons [3,7–9], which enhances the process at low intensities. As a light source, entangled photons can collectively excite uncoupled atoms [10,11], and lead to entanglement-induced two-photon transparency [9], which cannot be obtained by a classical laser source.

Typical sources of entangled photons use the process of spontaneous parametric down-conversion (SPDC) in nonlinear crystals in the visible and infrared region of the spectrum [12]. These sources generate energy-time entangled photons with correlation times on the femtosecond timescale which has been only recently directly measured [13]. SPDC has also been demonstrated in the hard x-ray regime where the correlation times are expected to be attoseconds or smaller [14]. Recent experiments using nanophotonic chips for SPDC have demonstrated entangled photon generation with broad bandwidth of 100 THz (0.41 eV) and a high generation efficiency of 13 GHz/mW [15]. Here, we propose a method to generate entangled photon pairs in the extreme-ultraviolet (XUV) regime with an ultrabroad energy bandwidth (>20 eV) large enough to create correlation times on the attosecond scale.

It is well known that the $1s2s\ ^1S_0$ metastable state of a helium atom, its isoelectronic ions, and the $2s\ ^2S_{1/2}$ metastable state of the helium ion decay predominantly by two-photon emission [16–20]. The emitted photons are energy-time entangled with a correlation time related to the energy spacing between the $2s$ and $1s$ levels which is 20.62 and 40.81 eV for the helium atom and ion, respectively. Two-photon emission as a source of energy-time entangled photons has been previously studied in semiconductors [21,22] where the energy bandwidth is small due to the small band gap. The large energy bandwidth of the emitted entangled photons from metastable helium and heliumlike ions corresponds to correlation times in the attosecond domain, thus opening up the possibility of attosecond timescale pump-probe experiments using these photons.

We first consider a gedanken experimental setup in which we have a spheroidal cavity containing two helium atoms, with one atom placed at each of its two foci. One of the atoms is prepared in the $1s2s\ (^1S_0)$ excited state, which is used as an emitter (atom 1), and the other atom is in $1s^2\ (^1S_0)$ ground state, which is used as an absorber (atom 2), as shown in Fig. 1. Atom 1 decays to the $1s^2$ ground state by the simultaneous emission of two photons, according to selection rules. This decay channel dominates over the magnetic dipole transition to the $1s2s\ ^3S_1$ state. The metastable $1s2s\ (^1S_0)$ state has a long lifetime of $\tau = 0.0197$ s [23], and the energy gap between the $1s2s\ (^1S_0)$ and $1s^2$ states is 20.62 eV. Thus, the two emitted photons have both a good frequency correlation and a narrow emission time difference. The biphotons

*wang3607@purdue.edu

†niranjan@purdue.edu

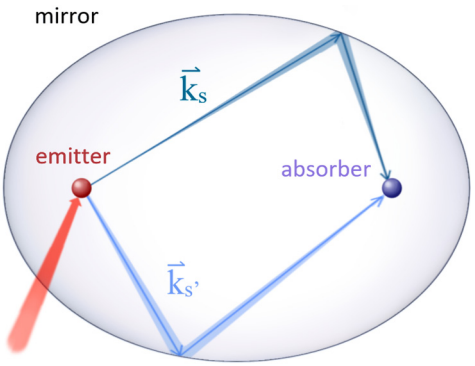

FIG. 1. A schematic diagram of entangled photon generation and absorption in a spheroidal cavity. The emission and absorption atoms are placed at the two foci of the spheroid. The photons are reflected by the boundary of the cavity, and propagate along equal length paths to reach the absorber. The shape of the cavity will influence the rate of this process by a geometry factor, as discussed in the Supplemental Material [25].

should also be correlated in angular momentum, according to the angular momentum conservation rule. However, we do not address that aspect, since inside a spheroidal cavity the entangled photon pair will be collected at the absorber after traveling along equal length paths, irrespective of their angular distribution or momenta. In treating this process we assume the following: (1) The cavity is large enough, that no quantization of photon frequencies or Purcell effect is relevant. (2) Both atoms are deeply trapped, so no recoil effects can be observed. (3) The mirror of the cavity is 100% reflective to all the frequencies, so no energy loss occurs during reflection of the photons. Further, it is noted that the emitted biphotons are also polarization entangled but we do not discuss polarization entanglement in this Letter. All possible polarization configurations are considered in our calculation. Our evaluations are based on a variational R-matrix calculation, which represents the atomic states as antisymmetrized products of single-electron orbitals, inside an R-matrix box radius of 34 a.u. The single-electron radial basis set includes functions with up to 38 nodes, and orbital angular momenta $l = 0$–9. The correlations between the electrons are fully accounted for in this approach. A detailed introduction of our method can be found in Ref. [24], which also demonstrates the accuracy of our calculation.

Inside the cavity, the photon-atom interaction takes place in three stages: the population inversion of atom 1, the spontaneous two-photon emission by atom 1, and photoabsorption by atom 2. In the first stage, we prepare the singlet $1s2s$ state using four-photon absorption, with photons of energy $\hbar\omega_0 = 5.155$ eV (240.54 nm). With a monochromatic incident electric field $\mathcal{E}_0\hat{\epsilon}_0\cos(\omega_0 t)$, the four-photon excitation amplitude $C_{\rm exc}$ is

$$C_{\rm exc}(t) = \left(\frac{e\mathcal{E}_0}{2\hbar}\right)^4 \frac{e^{i(\Delta_{eg}-4\omega_0)t}-1}{\Delta_{eg}-4\omega_0} D^{(4)}_{eg},$$
$$D^{(4)}_{eg} = \sum_{j_1,j_2,j_3} \frac{\langle e|\hat{\epsilon}_0\cdot\vec{r}|j_3\rangle\langle j_3|\hat{\epsilon}_0\cdot\vec{r}|j_2\rangle\langle j_2|\hat{\epsilon}_0\cdot\vec{r}|j_1\rangle\langle j_1|\hat{\epsilon}_0\cdot\vec{r}|g\rangle}{(\Delta_{j_3g}-3\omega_0)(\Delta_{j_2g}-2\omega_0)(\Delta_{j_1g}-\omega_0)}, \quad (1)$$

where $|g\rangle$ is the $1s^2$ ground and the initial state, $|e\rangle$ is the $1s2s$ excited and the final state, $|j_{1,2,3}\rangle$ are the intermediate states, and the Δ with indices are the energy difference between them. Equation (1) is given under the electric dipole approximation, with $\vec{r}$ representing the summed position space vectors of the two electrons, $\vec{r} = \vec{r}_1 + \vec{r}_2$. Through the following identity,

$$\lim_{t\to\infty} \frac{e^{i(\Delta_{eg}-4\omega_0)t}-1}{\Delta_{eg}-4\omega_0} = -\mathcal{P}\left(\frac{1}{\Delta_{eg}-4\omega_0}\right) + i\pi\delta(\Delta_{eg}-4\omega_0),$$

the resulting unnormalized state following the excitation, which is also the initial state for the emission process, is $|\gamma\rangle = i\pi\delta(\Delta_{eg}-4\omega_0)(\frac{e\mathcal{E}_0}{2\hbar})^4 D^{(4)}_{eg}|e\rangle$. For a realistic laser field, the δ function should be integrated over a broadened spectrum of the laser, as is discussed in the Supplemental Material [25].

The photon-atom interaction for the second and third stages is

$$V^{\rm int}(t) = e\vec{r}\cdot\vec{\mathcal{E}}(t),$$
$$\vec{\mathcal{E}}(t) = \sum_s i\hat{\epsilon}_s\left(\frac{2\pi\hbar\omega_s}{V}\right)^{\frac{1}{2}}\left(a_s e^{i(\vec{k}_s\cdot\vec{r}-\omega_s t)} - a_s^\dagger e^{-i(\vec{k}_s\cdot\vec{r}-\omega_s t)}\right), \quad (2)$$

where $\vec{\mathcal{E}}$ is the electric field of one emitted/reabsorbed photon, and V is the quantization volume. The electric field generated by a single photon is proportional to $1/\sqrt{V}$. The photon modes s have frequency ω_s, propagation direction $\hat{k}_s$, and polarization direction $\hat{\epsilon}_s$. From a second-order perturbation analysis, the amplitude of two-photon emission ($|\gamma\rangle\otimes|{\rm vac}\rangle \to |g\rangle\otimes|1_s, 1_{s'}\rangle$) is

$$C^{(s,s')}_{\rm emi}(t) = -\frac{2\pi e^2}{V}\sqrt{\omega_s\omega_{s'}}\frac{e^{i(\omega_s+\omega_{s'}-\Delta_{eg})t}-1}{\omega_s+\omega_{s'}-\Delta_{eg}} \times \sum_j \frac{\langle g|\hat{\epsilon}_{s'}\cdot\vec{r}|j\rangle\langle j|\hat{\epsilon}_s\cdot\vec{r}|\gamma\rangle}{\hbar(\omega_s-\Delta_{ej})}. \quad (3)$$

$|j\rangle$ denotes the intermediate states for the emission process. From Eq. (3) we obtain the He $1s2s$ ($^1S_0$) lifetime as $\tau = 0.0197$ s, which agrees with the experimental value [23].

Since no singlet energy level exists between E_i and $E_i + \Delta_{eg}$ for atom 2, the absorption process can only start after both photons have been emitted, with $\omega_s + \omega_{s'} = \Delta_{eg}$. The modes of the photons are not detectable inside the cavity, therefore the entangled photon state is obtained by summing over all

the modes (s, s') [26]:

$$|2\text{ph}\rangle = \sum_{s,s'} C_{\text{emi}}^{(s,s')}(t \to \infty)|1_s, 1_{s'}\rangle. \tag{4}$$

Based on a second-order perturbation calculation, the entangled photon absorption amplitude can be written as

$$C_{\text{abs}}(t) = -\frac{e^2}{\hbar^2}\int_0^t dt_2 \int_{-\infty}^{t_2} dt_1 \sum_m e^{i(\Delta_{mi}t_1+\Delta_{fm}t_2)} \times (\langle f| \otimes \langle \text{vac}|)\vec{r}\cdot\vec{\mathcal{E}}(t_2)|m\rangle\langle m|\vec{r}\cdot\vec{\mathcal{E}}(t_1)(|i\rangle \otimes |2\text{ph}\rangle). \tag{5}$$

$|i\rangle$, $|m\rangle$, and $|f\rangle$ denote the initial, intermediate, and final states for atom 2. $\vec{\mathcal{E}}(t_{1,2})$ in Eq. (5) are the electric fields of the photons that are reflected by the cavity (whose frequencies stay the same but propagation and polarization directions change), and absorbed at times t_1 and t_2, respectively. The evaluation of Eq. (5) depends on the shape of the cavity; the absorption process can be described by a rank-0 tensor, which is discussed in the Supplemental Material [25].

The time correlation of the entangled photon pair can be found from the scalar $\langle \text{vac}|\mathcal{E}(t_2)\mathcal{E}(t_1)|2\text{ph}\rangle$, which is proportional to the Fourier transformation of the spectrum [8,9,27], as

$$\langle \text{vac}|\mathcal{E}(t_2)\mathcal{E}(t_1)|2ph\rangle \propto \int_0^{\Delta_{eg}} d\omega_s e^{i\omega_s(t_2-t_1)}[\omega_s(\Delta_{eg}-\omega_s)]^3 \sum_j \left(\frac{\langle g|r|j\rangle\langle j|r|e\rangle}{\hbar(\omega_s-\Delta_{ej})} + \frac{\langle g|r|j\rangle\langle j|r|e\rangle}{\hbar(\Delta_{jg}-\omega_s)}\right). \tag{6}$$

The right-hand side of Eq. (6) is plotted in Fig. 2 against the time difference between absorption events of the two photons. The timescale between the two absorption events is around ±4 a.u., which gives a correlation time [5] around 200 as. Finally, according to Eqs. (1), (3), and (5), the rate of excitation, emission, and absorption, where an entangled photon pair is transferred coherently, is

$$R_{\text{trans}} = 2\pi\delta(\Delta_{fi}-\Delta_{eg})\left|\frac{\Theta e^8\mathcal{E}_0^4}{256\hbar^6c^6}D_{eg}^{(4)}\delta(\Delta_{eg}-4\omega_0)\int d\omega_s[\omega_s(\Delta_{eg}-\omega_s)]^3 \times \sum_{m\,j}\frac{\langle f|r|m\rangle\langle m|r|i\rangle}{\omega_s-\Delta_{mi}}\left(\frac{\langle g|r|j\rangle\langle j|r|e\rangle}{\omega_s-\Delta_{ej}}+\frac{\langle g|r|j\rangle\langle j|r|e\rangle}{\Delta_{jg}-\omega_s}\right)\right|^2. \tag{7}$$

Θ is a geometry factor which is introduced in Eq. (S3) and its values shown in Fig. S1 in the Supplemental Material [25]. Specifically, for a spherical cavity, $\Theta = \frac{64\pi^2}{27}$ and $R_{\text{trans}} = 1.91\times10^{-25}\mathcal{E}_0^8$ a.u. The input beam flux is $J = \frac{c\mathcal{E}_0^2}{8\pi\hbar\omega_0}$. Note that the transition rate is proportional to J^4. The entangled photon absorption rate is known to be proportional to the beam intensity (when the beam intensity is not very strong) [2,7,9], and our result can be regarded as a generalization of this linearity. Since our excitation process involves four photons, the four-photon flux can be considered the input flux, $J^{(4)} = J^4$, with $R_{\text{trans}} \propto J^{(4)}$.

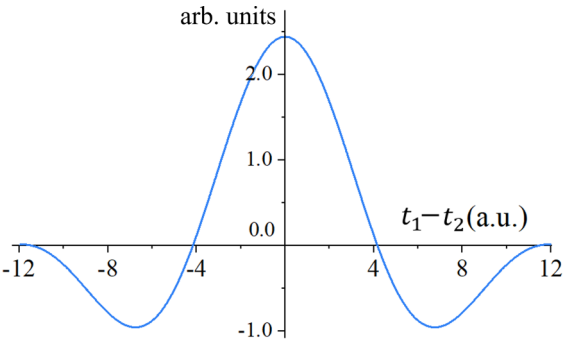

FIG. 2. The photon correlation function $\langle \text{vac}|\mathcal{E}(t_2)\mathcal{E}(t_1)|2\text{ph}\rangle$ (up to a constant factor) as a function of the time difference $t_2 - t_1$ (a.u.), which indicates that the correlation time is around 200 attoseconds (as).

The above calculations assume a direct multiphoton excitation from $1s^2$ to $1s2s$. Since the $1s2s\ ^1S_0$ metastable state has a narrow linewidth of ∼50 Hz, a multiphoton excitation to this state ideally requires intense lasers with a linewidth smaller than 50 Hz at a wavelength of 240 nm. While multiphoton excitations of metastable states with narrow linewidth lasers have been previously demonstrated [28], achieving the required high intensities with a narrow-band 240-nm laser is currently challenging. However, femtosecond lasers that can achieve peak intensities of 10^{14} W cm^{-2} are readily available. Using our calculations for the four-photon excitation rate with a monochromatic electric field, we estimate the helium $1s2s\ ^1S_0$ four-photon excitation rate for a femtosecond laser. With a 240-nm femtosecond laser, with a typical bandwidth of ∼5 THz, we obtain a biphoton generation rate of $\sim10^{11}$ s^{-1} [see Supplemental Material [25] and Fig. 3(a)].

An alternative scheme using a lambda-type transition between the $1s^2$, $1s2p$, and $1s2s$ states could be used to achieve significant excitation. The energy levels of the latter two are 21.22 and 20.62 eV above the ground state, respectively. A two-step sequential excitation to first excite the $1s^2 \to 1s2p$ transition and then the $1s2p \to 1s2s$ transition could be used. The oscillator strengths for the one-photon excitation processes are $f_{a\to b} = 2\Delta_{ba}|\langle b|\hat{\epsilon}_0\cdot\vec{r}|a\rangle|^2$, which gives $f_{1s^2\to1s2p} = 0.28$ and $f_{1s2p\to1s2s} = -0.36$ for the two steps. To achieve this two-step sequential excitation, a high photon flux helium lamp source can be used in the first step to excite $1s2p$ and a 2059-nm laser can transfer population to the $1s2s$ state [see Fig. 3(b)]. The ∼2 GHz linewidth of the $1s2p$ state makes transitions to the $1s2s$ state using a broadband laser

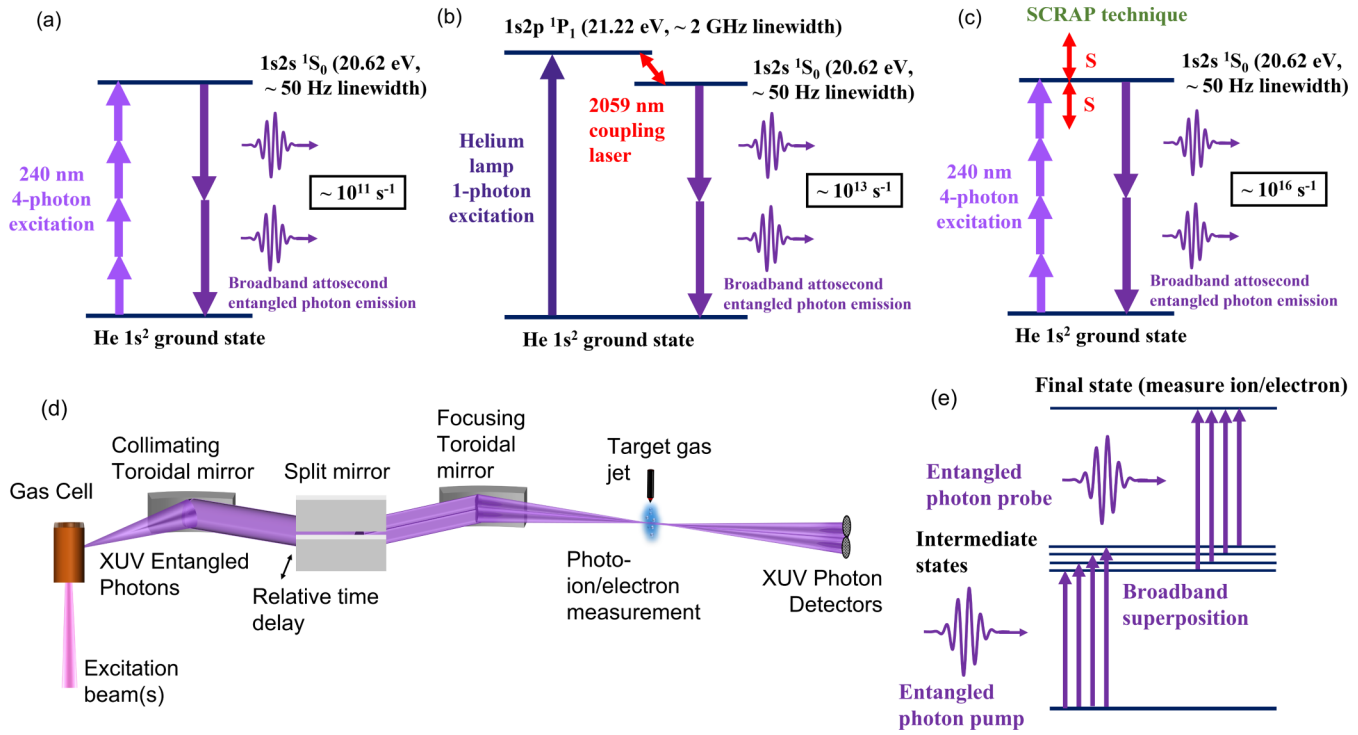

FIG. 3. (a) Generation of entangled biphotons in the XUV via two-photon decay of the $1s2s\ ^1S_0$ state excited by four-photon excitation using a broadband 240-nm laser. (b) Two-step sequential excitation of the $1s2s$ state via the $1s2p$ state using a high photon flux helium lamp and a 2059-nm coupling laser. (c) The SCRAP technique to populate the $1s2s$ state using a multiphoton pump pulse and a Stark shifting pulse which enable rapid adiabatic passage and ionization suppression by LICS (LICS not shown). The estimated biphoton generation rate is also shown for each scheme in (a)–(c). (d) Proposed experimental scheme to generate XUV entangled photons and utilize them in an attosecond pump-probe photoionization experiment. (e) An attosecond pump-probe photoionization scheme in molecules using entangled biphotons.

more feasible in comparison to direct multiphoton excitation. Currently available helium lamp sources are capable of generating $\sim 10^{15}$ photons s^{-1}. Using a high-pressure helium target, nearly all of these photons could be absorbed to generate helium atoms in the $1s2p$ state. A high repetition rate pulsed laser source at 2059 nm could transfer nearly all these excited helium atoms to the $1s2s$ state. We estimate a biphoton generation rate of $\sim 10^{13}$ s^{-1} using this method (see Supplemental Material [25]).

Another alternative approach to achieve significant population of the $1s2s$ singlet metastable state is to use Stark-chirped rapid adiabatic passage (SCRAP), previously proposed to excite the $2s$ metastable state in a hydrogen atom [29,30]. In this technique, a pump pulse excites the metastable state via a multiphoton transition in the presence of a Stark pulse that Stark shifts the $1s2s$ state across the bandwidth of the pump pulse [see Fig. 3(c)]. The combined effect of the two pulses results in a Landau-Zener-type adiabatic passage that can significantly populate the $1s2s$ state. The SCRAP technique [30] can also suppress ionization loss by laser-induced continuum structure (LICS) [31–33]. If we ignore ionization loss, for a typical femtosecond laser pulse width of 50 fs with a bandwidth of 8.8 THz, rapid adiabatic passage can excite nearly all atoms in the focal volume. When ionization loss is considered, since LICS can suppress ionization loss, it is reasonable to assume that $\sim 0.1\%$ of the atoms can be excited using SCRAP for every pair of pump and Stark pulses. With $\sim 10^{14}$ atoms in the focal volume corresponding to a 100 μm spot size and 1 mm path length at 1 bar target pressure, this results in $\sim 10^{11}$ atoms excited per pulse. At a femtosecond pulse repetition rate of 100 kHz currently available, this results in an entangled biphoton generation rate of 10^{16} s^{-1} (see Supplemental Material [25]). Among the three methods discussed here to excite helium to the singlet $1s2s$ state, the SCRAP method is expected to provide the highest excitation rate and hence the highest entangled biphoton generation rate.

The biphotons from the decay of the $1s2s$ state are emitted in all directions with an approximate distribution given by $1 + \cos^2(\theta)$ [20], where θ is the relative angle between the entangled photons. The photons that are emitted in a direction orthogonal to the excitation laser propagation direction can be collected within a large solid angle and sent along independent time-delayed paths towards a pump-probe target. Figure 3(d) shows a schematic of a proposed experimental setup for the generation of these entangled photons and their utilization in an attosecond pump-probe experiment. In this scheme, a grazing incidence toroidal mirror collimates the emitted photons which are then split into two halves using a grazing incidence split mirror that introduces a controllable time delay between the two halves of the beam. Collecting biphotons emitted along the same direction within a large solid angle (as opposed to those emitted in opposite directions) ensures that no time smearing is introduced in the arrival times of the biphotons. A 10% collection solid angle will result in 1% collection of biphotons. The split beams are then focused using a second toroidal mirror onto the target gas jet. A

pump-probe experiment with attosecond time resolution can be performed by measuring a photoion or photoelectron signal arising from the absorption of entangled biphotons by an atom or molecule [see Fig. 3(e)]. Recent work on entangled two-photon absorption sets upper bounds on the enhancements in a two-photon absorption cross section with entangled photons when no intermediate resonances are involved [34,35]. Assuming a biphoton rate of $\sim 10^{12}$ s^{-1} at the pump-probe target and a two-photon cross section of 10^{-50} cm^4 s, a pump-probe photoionization rate of ~1000 ions per second, which is well above the detection threshold of ion spectrometers, is expected. When intermediate resonances are involved, such as broad absorption resonances in molecules typically studied in attosecond experiments, this photoionization rate can be increased by a few orders of magnitude (see Supplemental Material [25]). Further, measuring a pump-probe photoionization signal as opposed to a photon absorption signal as in previous two-photon absorption experiments allows for the detection of low absorption rates. Such entangled photon pump-probe experiments will extend the capabilities of attosecond science, where currently attosecond pulses from high-order harmonic generation (HHG) [36] or free-electron laser [37] sources are used.

The entangled photon generation schemes discussed here can be extended to the soft x-ray (SXR) regime using heliumlike ions. Two-photon decay in heliumlike ions has been well studied [16,18,20]. Similar to the $1s2s\ ^1S_0$ state of neutral helium atoms, the $1s2s\ ^1S_0$ states of heliumlike ions such as N^{5+}, O^{6+}, and Ne^{8+}, predominantly decay by two-photon emission with a rate proportional to Z^6, where Z is the atomic number. The large energy difference between such excited states and the ground state of the ions, which can be in the range of several hundred to thousands of eV, results in entangled photon correlation times of a few attoseconds to zeptoseconds. For example, the $1s2s\ ^1S_0$ state of Ne^{8+} is located ~915 eV above the Ne^{8+} ground state and this bandwidth corresponds to an entangled photon correlation time of ~5 as. The two-photon decay rate in this case is $\sim 1\times 10^7$ s^{-1} which is significantly larger than the corresponding rate for neutral helium atoms of $\sim 5\times 10^1$ s^{-1}. Ne^{8+} has been previously generated using strong femtosecond laser fields [38,39] as well as using strong femtosecond x-ray pulses from free-electron lasers (FELs) [40] both of which can potentially also create Ne^{8+} in the $1s2s\ ^1S_0$ excited state. In one possible scheme, strong laser field ionization could generate Ne^{8+} ions in the ground state and an FEL could excite them to the $1s2s\ ^1S_0$ state by two-photon excitation which then generates highly broadband entangled biphotons at SXR energies. It has been previously demonstrated experimentally that the bandwidth required to generate few-attosecond pulses can be obtained from HHG using midinfrared pulses [41]. Further, it has been theoretically shown that zeptosecond pulses can be generated from HHG when suitable filters are used [42]. However, the shortest measured attosecond pulse is currently 43 as [36]. Our approach of using entangled photons from the two-photon decay of heliumlike ions offers an alternative path for carrying out ultrafast measurements in these extreme regimes of a few attoseconds to zeptoseconds.

In conclusion, an unconventional approach is presented here for generating attosecond entangled biphotons in the XUV and SXR regimes using two-photon decay in helium atoms and heliumlike ions. Multiple alternative schemes can be used to excite the $1s2s\ ^1S_0$ metastable state in helium for which excitation rates have been estimated and an experimental scheme is suggested to collect and use the emitted XUV biphotons in attosecond pump-probe experiments. The calculated photoionization rates indicate that attosecond pump-probe experiments with entangled photons are feasible. A potential extension of such metastable excitations to heliumlike ions is additionally proposed, whereby SXR biphotons can be generated with entanglement times in the few-attosecond range with the possibility of reaching the zeptosecond regime. This approach can open doors to using XUV/SXR entangled photons in quantum imaging and attosecond quantum spectroscopy of atomic, molecular, and solid-state systems.

The work of C.H.G. and Y.W. is supported by the U.S. Department of Energy, Office of Science, Basic Energy Sciences, under Award No. DE-SC-0010545.

[1] R. Horodecki, P. Horodecki, M. Horodecki, and K. Horodecki, Quantum entanglement, Rev. Mod. Phys. **81**, 865 (2009).

[2] D.-I. Lee and T. Goodson, Entangled photon absorption in an organic porphyrin dendrimer, J. Phys. Chem. B **110**, 25582 (2006).

[3] F. Schlawin, K. E. Dorfman, and S. Mukamel, Entangled two-photon absorption spectroscopy, Acc. Chem. Res. **51**, 2207 (2018).

[4] B. E. A. Saleh, B. M. Jost, H.-B. Fei, and M. C. Teich, Entangled-Photon Virtual-State Spectroscopy, Phys. Rev. Lett. **80**, 3483 (1998).

[5] D. Strekalov, A. B. Matsko, A. A. Savchenkov, and L. Maleki, Relationship between quantum two-photon correlation and classical spectrum of light, Phys. Rev. A **71**, 041803(R) (2005).

[6] P. Pfeifer and J. Fröhlich, Generalized time-energy uncertainty relations and bounds on lifetimes of resonances, Rev. Mod. Phys. **67**, 759 (1995).

[7] K. E. Dorfman, F. Schlawin, and S. Mukamel, Nonlinear optical signals and spectroscopy with quantum light, Rev. Mod. Phys. **88**, 045008 (2016).

[8] J. Peřina, B. E. A. Saleh, and M. C. Teich, Multiphoton absorption cross section and virtual-state spectroscopy for the entangled n-photon state, Phys. Rev. A **57**, 3972 (1998).

[9] H.-B. Fei, B. M. Jost, S. Popescu, B. E. A. Saleh, and M. C. Teich, Entanglement-Induced Two-Photon Transparency, Phys. Rev. Lett. **78**, 1679 (1997).

[10] A. Muthukrishnan, G. S. Agarwal, and M. O. Scully, Inducing Disallowed Two-Atom Transitions with Temporally Entangled Photons, Phys. Rev. Lett. **93**, 093002 (2004).

[11] M. Richter and S. Mukamel, Collective two-particle resonances induced by photon entanglement, Phys. Rev. A **83**, 063805 (2011).

[12] P. G. Kwiat, K. Mattle, H. Weinfurter, A. Zeilinger, A. V. Sergienko, and Y. Shih, New High-Intensity Source of

Polarization-Entangled Photon Pairs, Phys. Rev. Lett. **75**, 4337 (1995).

[13] J.-P. W. MacLean, J. M. Donohue, and K. J. Resch, Direct Characterization of Ultrafast Energy-Time Entangled Photon Pairs, Phys. Rev. Lett. **120**, 053601 (2018).

[14] S. Sofer, E. Strizhevsky, A. Schori, K. Tamasaku, and S. Shwartz, Quantum Enhanced X-ray Detection, Phys. Rev. X **9**, 031033 (2019).

[15] U. A. Javid, J. Ling, J. Staffa, M. Li, Y. He, and Q. Lin, Ultrabroadband Entangled Photons on a Nanophotonic Chip, Phys. Rev. Lett. **127**, 183601 (2021).

[16] A. T. Bondy, D. C. Morton, and G. W. F. Drake, Two-photon decay rates in heliumlike ions: Finite-nuclear-mass effects, Phys. Rev. A **102**, 052807 (2020).

[17] M. Lipeles, R. Novick, and N. Tolk, Direct Detection of Two-Photon Emission from the Metastable State of Singly Ionized Helium, Phys. Rev. Lett. **15**, 690 (1965).

[18] G. W. Drake, G. Victor, and A. Dalgarno, Two-photon decay of the singlet and triplet metastable states of helium-like ions, Phys. Rev. **180**, 25 (1969).

[19] M. Prior, Lifetime of the 2*S* State of He^+, Phys. Rev. Lett. **29**, 611 (1972).

[20] P. H. Mokler and R. W. Dunford, Two-photon decay in heavy atoms and ions, Phys. Scr. **69**, C1 (2004).

[21] A. Hayat, P. Ginzburg, and M. Orenstein, High-rate entanglement source via two-photon emission from semiconductor quantum wells, Phys. Rev. B **76**, 035339 (2007).

[22] A. Hayat, P. Ginzburg, and M. Orenstein, Observation of two-photon emission from semiconductors, Nat. Photon. **2**, 238 (2008).

[23] R. S. Van Dyck, C. E. Johnson, and H. A. Shugart, Radiative lifetime of the $2\,^1S_0$ metastable state of helium, Phys. Rev. A **4**, 1327 (1971).

[24] Y. Wang and C. H. Greene, Two-photon above-threshold ionization of helium, Phys. Rev. A **103**, 033103 (2021).

[25] See Supplemental Material at http://link.aps.org/supplemental/10.1103/PhysRevResearch.4.L032038 for details on the calculation of the geometry factor for the spheroid cavity, estimates for the entangled biphoton generation rates in various schemes, and estimates for photoionization rates from entangled two-photon absorption in an attosecond pump-probe experiment.

[26] Y. Shih, Entangled biphoton source - property and preparation, Rep. Prog. Phys. **66**, 1009 (2003).

[27] U. M. Titulaer and R. J. Glauber, Correlation functions for coherent fields, Phys. Rev. **140**, B676 (1965).

[28] C. G. Parthey, A. Matveev, J. Alnis, B. Bernhardt, A. Beyer, R. Holzwarth, A. Maistrou, R. Pohl, K. Predehl, T. Udem *et al.*, Improved Measurement of the Hydrogen 1*S*–2*S* Transition Frequency, Phys. Rev. Lett. **107**, 203001 (2011).

[29] L. P. Yatsenko, B. W. Shore, T. Halfmann, K. Bergmann, and A. Vardi, Source of metastable H(2*s*) atoms using the Stark chirped rapid-adiabatic-passage technique, Phys. Rev. A **60**, R4237 (1999).

[30] L. P. Yatsenko, V. R. Romanenko, B. W. Shore, T. Halfmann, and K. Bergmann, Two-photon excitation of the metastable 2*s* state of hydrogen assisted by laser-induced chirped Stark shifts and continuum structure, Phys. Rev. A **71**, 033418 (2005).

[31] P. L. Knight, M. Lauder, and B. J. Dalton, Laser-induced continuum structure, Phys. Rep. **190**, 1 (1990).

[32] T. Halfmann, L. P. Yatsenko, M. Shapiro, B. W. Shore, and K. Bergmann, Population trapping and laser-induced continuum structure in helium: Experiment and theory, Phys. Rev. A **58**, R46 (1998).

[33] L. P. Yatsenko, T. Halfmann, B. W. Shore, and K. Bergmann, Photoionization suppression by continuum coherence: Experiment and theory, Phys. Rev. A **59**, 2926 (1999).

[34] T. Landes, M. G. Raymer, M. Allgaier, S. Merkouche, B. J. Smith, and A. H. Marcus, Quantifying the enhancement of two-photon absorption due to spectral-temporal entanglement, Opt. Express **29**, 20022 (2021).

[35] T. Landes, M. Allgaier, S. Merkouche, B. J. Smith, A. H. Marcus, and M. G. Raymer, Experimental feasibility of molecular two-photon absorption with isolated time-frequency-entangled photon pairs, Phys. Rev. Research **3**, 033154 (2021).

[36] T. Gaumnitz, A. Jain, Y. Pertot, M. Huppert, I. Jordan, F. Ardana-Lamas, and H. J. Wörner, Streaking of 43-attosecond soft-x-ray pulses generated by a passively CEP-stable mid-infrared driver, Opt. Express **25**, 27506 (2017).

[37] J. Duris, S. Li, T. Driver, E. G. Champenois, J. P. MacArthur, A. A. Lutman, Z. Zhang, P. Rosenberger, J. W. Aldrich, R. Coffee *et al.*, Tunable isolated attosecond x-ray pulses with gigawatt peak power from a free-electron laser, Nat. Photon. **14**, 30 (2020).

[38] J. K. Crane, T. Ditmire, H. Nguyen, and M. D. Perry, Observation of strong emission from Ne IX and Ne X transitions in a laser-driven plasma, in *The 4th International Colloquium: X-Ray Lasers 1994*, edited by D. C. Eder and D. L. Matthews, AIP Conf. Proc. Vol. 332 (AIP, Woodbury, NY, 1995), p. 253.

[39] E. A. Chowdhury and B. C. Walker, Multielectron ionization processes in ultrastrong laser fields, J. Opt. Soc. Am. B **20**, 109 (2003).

[40] L. Young, E. P. Kanter, B. Kraessig, Y. Li, A. March, S. Pratt, R. Santra, S. Southworth, N. Rohringer, L. DiMauro *et al.*, Femtosecond electronic response of atoms to ultra-intense x-rays, Nature (London) **466**, 56 (2010).

[41] T. Popmintchev, M.-C. Chen, D. Popmintchev, P. Arpin, S. Brown, S. Ališauskas, G. Andriukaitis, T. Balčiunas, O. D. Mücke, A. Pugzlys *et al.*, Bright coherent ultrahigh harmonics in the keV x-ray regime from mid-infrared femtosecond lasers, Science **336**, 1287 (2012).

[42] C. Hernández-García, J. A. Pérez-Hernández, T. Popmintchev, M. M. Murnane, H. C. Kapteyn, A. Jaron-Becker, A. Becker, and L. Plaja, Zeptosecond High Harmonic keV X-Ray Waveforms Driven by Midinfrared Laser Pulses, Phys. Rev. Lett. **111**, 033002 (2013).